AGU PUBLICATIONS

Water Resources Research

RESEARCH ARTICLE
10.1002/2016WR018930

Key Points:
- Three-dimensional multicomponent solute transport model parameterization
- Multicomponent solute transport in drip-irrigated lysimeters
- Lysimeter design effects on leaching fractions and ESP

Supporting Information:
- Supporting Information S1

Correspondence to:
N. Lazarovitch,
lazarovi@bgu.ac.il

Citation:
Raij, I., J. Šimůnek, A. Ben-Gal, and N. Lazarovitch (2016), Water flow and multicomponent solute transport in drip-irrigated lysimeters, *Water Resour. Res.*, *52*, doi:10.1002/2016WR018930.

Received 15 MAR 2016
Accepted 7 AUG 2016
Accepted article online 16 AUG 2016

Water flow and multicomponent solute transport in drip-irrigated lysimeters

Iael Raij[1], Jiří Šimůnek[2], Alon Ben-Gal[3], and Naftali Lazarovitch[1]

[1]Wyler Department of Dryland Agriculture, French Associates Institute for Agriculture and Biotechnology of Drylands, Jacob Blaustein Institutes for Desert Research, Ben-Gurion University of the Negev, Sede Boqer Campus, Midreshet Ben-Gurion, Israel, [2]Department of Environmental Sciences, University of California, Riverside, Negev, California, USA, [3]Institute of Soil, Water and Environmental Sciences, Agricultural Research Organization, Gilat Research Center, Israel

Abstract Controlled experiments and modeling are crucial components in the evaluation of the fate of water and solutes in environmental and agricultural research. Lysimeters are commonly used to determine water and solute balances and assist in making sustainable decisions with respect to soil reclamation, fertilization, or irrigation with low-quality water. While models are cost-effective tools for estimating and preventing environmental damage by agricultural activities, their value is highly dependent on the accuracy of their parameterization, often determined by calibration. The main objective of this study was to use measured major ion concentrations collected from drip-irrigated lysimeters to calibrate the variably saturated water flow model HYDRUS (2D/3D) coupled with the reactive transport model UNSATCHEM. Irrigation alternated between desalinated and brackish waters. Lysimeter drainage and soil solution samples were collected for chemical analysis and used to calibrate the model. A second objective was to demonstrate the potential use of the calibrated model to evaluate lower boundary design options of lysimeters with respect to leaching fractions determined using drainage water fluxes, chloride concentrations, and overall salinity of drainage water, and exchangeable sodium percentage (ESP) in the profile. The model showed that, in the long term, leaching fractions calculated with electrical conductivity values would be affected by the lower boundary condition pressure head, while those calculated with chloride concentrations and water fluxes would not be affected. In addition, clear dissimilarities in ESP profiles were found between lysimeters with different lower boundary conditions, suggesting a potential influence on hydraulic conductivities and flow patterns.

1. Introduction

A decrease in the availability of freshwater resources and an increase in food demand have led to the widespread utilization of lower-quality water for irrigation. The use of water with high salt concentrations necessitates irrigation in amounts higher than actual evapotranspiration (*ET*) in order to prevent soil salinization and subsequent yield loss [*Rawlins*, 1973]. Traditionally, irrigation water requirements, designed to minimize the negative effects of salinity on crop growth and yield when irrigating with brackish or high-salinity water, are determined by multiplying potential *ET* by a crop/cover factor and dividing by one minus a leaching fraction [*Allen et al*., 1998; *Corwin et al*., 2007; *Dudley et al*., 2008a]. This approach is problematic for real-time scheduling of crop irrigation for a number of reasons. Miscalculations and high daily variability of ET or timing and magnitude of rain events can lead to inefficient use of water and fertilizers, resulting in economic losses and to groundwater pollution from leached agrochemicals [*Oren et al*., 2004; *Corwin et al*., 2007]. Leaching fractions are commonly based on crop response functions determined for an entire season and average root zone salinity, which may not be relevant for all actual temporal or spatial field conditions [*Letey et al*., 2011; *Groenveld et al*., 2013]. Crop factors have additionally been shown to be sensitive to a reduction in transpiration due to salinity and other types of stresses [*Rhoades et al*., 1992; *Bhantana and Lazarovitch*, 2010]. Negative effects from these shortcomings can be minimized by scheduling irrigation and fertilization based on in situ monitoring of water and solute balances and by using pressurized irrigation systems, which allow frequent automated applications. Fertigation via drip systems has been shown to increase the efficiency of water and fertilizer applications [e.g., *Hanson et al*., 2006], to reduce salinity and drought stress in the root zone [e.g., *Hanson et al*., 2008], and to prevent leaching of fertilizers and agrochemicals into the groundwater [*Rhoades et al*., 1992; *Hartz and Hochmuth*, 1996].

In situ monitoring of salts, fertilizers, and other contaminants leaching into deep layers of the soil profile can provide information for improved decision making with respect to efficient and sustainable irrigation practices. Monitoring techniques include soil solution sampling with suction devices [*Rhoades et al*., 1999; *Corwin*, 2002; *Weihermüller et al*., 2007; *Wang et al*., 2012; *Turkeltaub et al*., 2015], destructive soil sampling and analysis, soil salinity sensors [*Vanclooster et al*., 1995; *Rhoades et al*., 1999], and lysimeters [*Bergström*, 1990]. Lysimeters isolate a volume of soil from its surroundings and allow monitoring of drainage amount and composition. The water and solute balances in lysimeters are obtained by monitoring exactly how much water and solutes enter, exit, and remain in the system. Lysimeters are commonly used in both the laboratory and the field to estimate the fate of pesticides and herbicides [*Winton and Weber*, 1996; *Schoen et al*., 1999]. Lysimeters are also widely used to determine crop factors (K_c) [*Marek et al*., 2006; *Bhantana and Lazarovitch*, 2010; *Bryla et al*., 2010] for irrigation scheduling based on meteorological data.

Monitoring of the chemical composition of drainage and solute loads allows the use of lysimeters as management tools for fertigation scheduling [*Ruiz-Peñalver et al*., 2015] and salt leaching [*Tripler et al*., 2012]. However, the boundary condition at the bottom of a lysimeter may limit or otherwise influence water flow and solute transport and thus, subsequently, water drainage and salt leaching into the underlying soil profile [*Flury et al*., 1999; *Ben-Gal and Shani*, 2002].

Lysimeters are generally categorized into two groups according to their lower boundary condition (LBC) and drainage collection method [*Bergström*, 1990]. First, free-drainage lysimeters are characterized by an atmospheric pressure at the bottom of the lysimeter, with drainage from them occurring only when saturation is reached. Studies comparing solute transport in free-drainage lysimeters and under field conditions reported differences not only due to the LBC but also in relation to soil texture, water fluxes, pore water velocity, soil heterogeneity, and sorption [*Flury et al*., 1999; *Gasser et al*., 2002; *Abdou and Flury*, 2004]. Two-dimensional numerical simulations showed that bromide moved faster in free-drainage lysimeters than in the field when lysimeters contained soil with vertical heterogeneities rather than with horizontal or isotropic heterogeneities [*Abdou and Flury*, 2004]. Numerical experiments reported by *Flury et al*. [1999] also showed that the coarser the soil and/or the smaller the water flux, the more pronounced the differences in the breakthrough of solutes between lysimeters and the field. This effect is due to the higher water contents in the lysimeter profile and therefore lower pore water velocities.

Second, suction-controlled lysimeters prevent saturated conditions at the lower soil boundary by applying a negative pressure head. Suction lysimeters can be either active or passive. Active suction-controlled lysimeters allow application of the pressure head, equivalent to that measured by a tensiometer under field conditions, at the bottom boundary [e.g., *Hannes et al*., 2015; *Groh et al*., 2016]. This type of lysimeter has high installation and maintenance costs and is difficult to repair when malfunctioning [*Bergström*, 1990].

In passive suction-controlled lysimeters, highly conductive media is used to connect the soil at the bottom of the lysimeter with the lysimeter's drainage exit and to extend it below this point [*Ben-Gal and Shani*, 2002]. These extensions hydraulically deepen the soil using a relatively small volume of material and move the saturated conditions to the end of the extensions themselves. The extensions are designed to not influence water flow in and from the soil above, and to maintain water content in the lysimeters similar to that expected in the soil profile under natural field conditions. This allows the use of a shallower soil component in lysimeters for agricultural research, simplifying installation and operation. While the effects of different lysimeter LBCs on water flow as a function of soil hydraulic properties are well understood [*Ben-Gal and Shani*, 2002], effects on drainage water composition or on dissolved and adsorbed solute distribution in the profile are not well understood and need to be further explored. It should be taken into account that in both passive and active suction-controlled lysimeters, materials used to apply the lower boundary suction may react with dissolved salts in the drainage solution [*Bergström*, 1990; *Weihermüller et al*., 2007].

Models can be cost-effective tools for evaluating and consequently preventing environmental damage by agricultural activities. However, model accuracy and reliability are highly influenced by the quality of their parameterization, often determined by calibration and validation [*Roberts et al*., 2009; *Ramos et al*., 2011; *Skaggs et al*., 2014]. Using replicated lysimeters for calibration of transport models is a good compromise between the accuracy of laboratory columns and the representativeness of field measurements [*Skaggs et al*., 2012]. Models such as HYDRUS-1D [*Šimůnek et al*., 2008] coupled with UNSATCHEM [*Suarez and Šimůnek*, 1997] have often been used to assess the implications and risks arising from various agricultural

practices such as irrigation with low-quality water in arid and semiarid regions [*Gonçalves et al*., 2006; *Kaledhonkar and Keshari*, 2006; *Ramos et al*., 2011; *Rasouli et al*., 2012; *Skaggs et al*., 2014]. However, the use of one-dimensional models to represent three-dimensional patterns created under drip irrigation may lead to erroneous conclusions [*Skaggs et al*., 2004; *Warrick and Lazarovitch*, 2007; *Chen et al*., 2010]. Evaluation of the reliability of lysimeters for monitoring solute leaching from agricultural lands irrigated with brackish water is expected to benefit from multidimensional solute transport and water movement modeling that considers various reactive processes, such as cation exchange and/or precipitation/dissolution.

The development of the UNSATCHEM module for the HYDRUS (2D/3D) software [*Šimůnek et al*., 2012], which allows consideration of water flow and solute transport with complex major ion chemistry in unsaturated conditions, has opened a window to explore the effects of the LBC on the quality of drainage from lysimeters and the distribution of ions in the soil profile of the lysimeter. This solution takes into consideration the complex interactions between the soil matrix and the major ions in the soil.

The objectives of this study thus were (a) to carry out water flow and solute transport experiments involving drip irrigation with brackish and desalinated water in lysimeter systems, (b) to use collected experimental data to calibrate the three-dimensional flow and transport model HYDRUS (2D/3D) [*Šimůnek et al*., 2008] coupled with the reactive transport model UNSATCHEM [*Šimůnek et al*., 2012], and (c) to use the calibrated three-dimensional reactive transport model to evaluate possible design options for the bottom boundary in lysimeters and their effects on (1) transient leaching fractions defined by the daily ratio of drainage and irrigation, either by volume, electrical conductivity, or chloride concentration and (2) spatial ESP (exchangeable sodium percentage) profiles in the lysimeter.

2. Experiments

2.1. Laboratory Column Experiments for Estimating Soil Retention Curve Parameters

A 0.85 m long PVC column with a diameter of 0.15 m was filled with loamy sand soil in intervals of 5 cm in order to maintain the same bulk density as in the lysimeters. The column was slowly wetted from below and once saturated a pressure head of $h = 0$ was imposed as the LBC using a Mariotte bottle. In addition, the top of the column was covered to prevent any evaporation. Once equilibrium was achieved, the column was opened and soil samples were taken every 5 cm and then oven dried for gravimetric water content calculation. In addition, a tensiometer-like device was filled with a known volume of oven dried loamy sand soil. This device consisted of a plastic cylinder 0.3 m long and a diameter of 0.02 m, with a ceramic cup at the lower boundary and a connection to pressurized nitrogen gas at the upper boundary. The device was saturated with water from below and then a pressure of 0.5 bar was applied at the top until equilibrium was reached, followed by another pressure application of 0.8 bar until equilibrium was reached again. Equilibrium was determined by weighing the device until its mass was stable and the gravimetric water content of the soil in the device was calculated. During this stage, the ceramic cup was covered with a plastic film to prevent evaporation.

2.2. Lysimeter Experiments

Water flow and solute transport experiments were conducted in an automated rotating lysimeter system [*Lazarovitch et al*., 2006], located in a greenhouse at The Jacob Blaustein Institutes for Desert Research, Sede Boqer Campus, Israel. The system consisted of eight lysimeters located in a circular arrangement. All lysimeters had the same surface area (0.70 m length and 0.35 m width) but four of them had a depth of 0.5 m and the other four had a depth of 0.25 m. The shallow lysimeters were used for the calibration of the Gapon exchange parameters and the deep lysimeters for the model validation. Each lysimeter had an independent automated irrigation delivery system and drainage collection system, and was located on a load cell for continuous weighing. The system rotated at two revolutions per hour and automatically stopped for either a scheduled irrigation application or drainage collection when a lysimeter was positioned at the irrigation/drainage collection station. All lysimeters were filled with loamy sand soil. Leachate flowed through two extensions (0.4 m long and 5 cm diameter) filled with rockwool [*Ben-Gal and Shani*, 2002] into a 0.0065 m^3 collection container. The two extensions were located at $X = 17.5$ cm and $Y = 25$ and 45 cm, respectively. Lysimeter geometry and drainage extension locations are described in Figure 1. Evaporation was prevented by plastic sheeting placed on the soil surface. The plastic mulch was covered with 2 cm of dry soil to minimize temperature variations. In each lysimeter, a ceramic suction sampling device (a ceramic cup, 6 cm

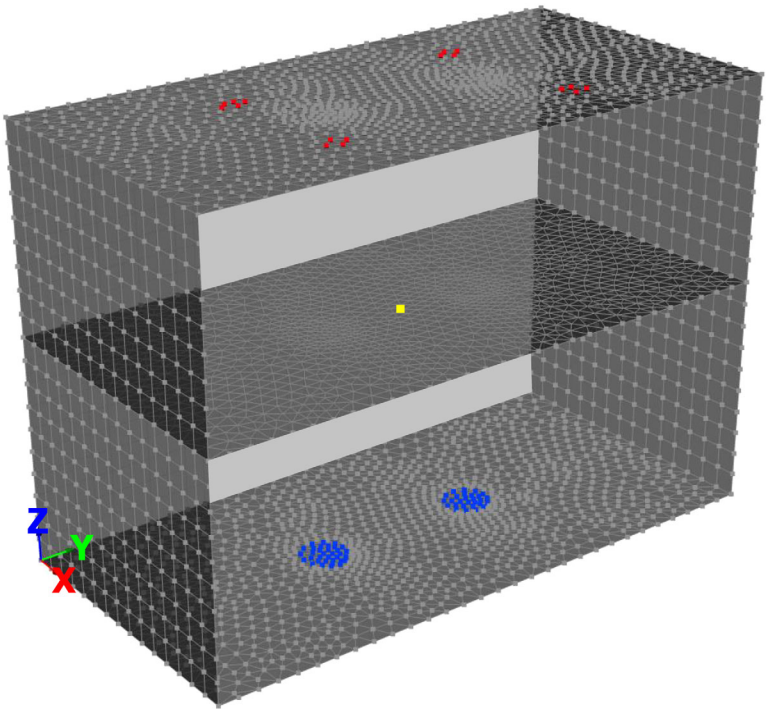

Figure 1. A schematic showing the simulated transport domain representing the lysimeter (0.7 m length, 0.35 m width, 0.5 m depth) in a rotating lysimeter system, finite element nodes, and the boundary conditions used in HYDRUS (2D/3D). Gray nodes are those with a no-flow boundary condition (BC), red nodes are those with a time-variable flux BC (top boundary), and blue nodes are those with a seepage face BC (bottom boundary). The yellow point represents the soil solution suction device.

long and 1.5 cm in diameter) was located in the middle of the container at depths of 0.25 and 0.125 m in deep and shallow lysimeters, respectively, to collect pore water samples every 2 or 3 days.

One liter of irrigation solution was applied twice daily to each lysimeter via four nonpressure compensated drippers (2 L h^{-1}, Netafim, Israel). To ensure similar initial conditions, low-salinity water (DW in Table 1) was applied first for 60 days until a constant drainage electrical conductivity (EC) was obtained in all lysimeters. During the second step, irrigation with brackish groundwater (GW in Table 1) was applied for 6 days. The time period of brackish water application was followed by low-salinity water irrigation until a condition of steady state was again reached regarding the EC of the drainage water. Drainage mass was measured automatically twice a day. Drainage water was manually sampled every 1 or 2 days, and the soil solution from the ceramic suction sampling device was collected every other weekday. Samples from the drainage and soil pore solutions were analyzed for EC by means of a Multimeter MM 40+, Crison; for sodium, magnesium, calcium, potassium, and sulfate concentrations by inductively coupled plasma emission spectrophotometry (ICP); and for chloride concentration by Chloride Analyzer (926, Sherwood).

3. Multicomponent Solute Transport: HYDRUS (2D/3D) Coupled With UNSATCHEM

Advective-dispersive chemical transport under transient water flow conditions in a partially saturated porous medium is described in the model as follows [*Šimůnek et al.*, 2012]:

Table 1. Irrigation Water Composition: GW Is Brackish Groundwater and DW Is Desalinated Water[a]

	$[Ca^{2+}]$	$[Mg^{2+}]$	$[Na^{+}]$	$[K^{+}]$	$[SO_4^{2-}]$	$[Cl^{-}]$	Measured EC (dS m^{-1})	EC From Cations (dS m^{-1})
GW	10.13	9.76	13.89	0.33	7.81	22.67	3.7	3.4
DW	1.72	0.38	1.52	0.02	1.08	1.37	0.36	0.36

[a]Units are in meq L^{-1} unless indicated otherwise. EC is electrical conductivity.

$$\frac{\partial \theta c_k}{\partial t}+\rho_b \frac{\partial \bar{c}_k}{\partial t}+\rho_b \frac{\partial \hat{c}_k}{\partial t}=\frac{\partial}{\partial x_i}\left(\theta D_{ij}\frac{\partial c_k}{\partial x_j}\right)-\frac{\partial q_i c_k}{\partial x_i}\quad k=1,2,\ldots,N_c, \tag{1}$$

where c_k is the total dissolved concentration of the component k [ML^{-3}], $\bar{c}_k$ is the total sorbed concentration of the component k [MM^{-1}], $\hat{c}_k$ is the total concentration of the component k in the minerals, which can precipitate or dissolve [MM^{-1}], ρ_b is the bulk density of the soil [ML^{-3}], D_{ij} is the dispersion coefficient tensor [$L^2\,T^{-1}$], i and j are spatial dimensions, q_i is the volumetric water flux [LT^{-1}] ($q_i = u_i\ \theta$,where u is the pore water velocity), θ is the volumetric water content [$L^3\,L^{-3}$] and N_c is the number of aqueous components. The dispersion coefficient tensor in the liquid phase, D_{ij}, is given by *Bear* [1972]:

$$\theta D_{ij}=\lambda_T|q|\delta_{ij}+(\lambda_L-\lambda_T)\frac{q_j q_i}{|q|}+\theta D_w \tau_w \delta_{ij}, \tag{2}$$

where λ_L and λ_T are the longitudinal and transverse dispersivities, respectively [L], δ_{ij} is the Kronecker delta function ($\delta_{ij} = 1$ if $i = j$, and $\delta_{ij} = 0$ if $i \neq j$), D_w is the molecular diffusion coefficient [$L^2\,T^{-1}$], and $\tau_w$is a tortuosity factor in the liquid phase.

Cation exchange between aqueous and exchangeable phases is described using the Gapon equation, under the assumption that the cation exchange capacity is constant and independent of pH [*Šimůnek et al*., 2012]:

$$K_{ij}=\frac{\bar{c}_i^{y+}\left(c_j^{x+}\right)^{1/x}}{\bar{c}_j^{x+}\left(c_i^{y+}\right)^{1/y}}, \tag{3}$$

where K_{ij} is the Gapon selectivity (K_G) coefficient, y and x are the valences of species i and j, respectively, $\bar{c}$ is the exchangable concentration in $mmol_c\ kg^{-1}$ of soil, and c is the soluble concentration in $mmol_c\ L^{-1}$. When all four cations (Mg^{2+}, Ca^{2+}, Na^{+}, and K^{+}) considered by UNSATCHEM are present, three Gapon coefficients for cation pairs Mg/Ca, Ca/Na, and Ca/K are needed.

Calcite and gypsum precipitation and dissolution are described by equilibrium equations (equations (4) and (5)) in the presence of CO_2. The UNSATCHEM module also includes precipitation and dissolution of nesquehonite, hydromagnesite, and sepiolite which were not included in this work.

$$CaSO_4 \cdot 2H_2O \rightleftarrows Ca^{2+}+SO_4^{2-}+2H_2O, \tag{4}$$

$$CaCO_3+CO_2(g)+H_2O \rightleftarrows Ca^{2+}+2HCO_3^{-}. \tag{5}$$

The solubility products K_{SP}^G[$meq^4\,L^{-4}$] and K_{SP}^C [$meq^2\,L^{-2}$] for gypsum and calcite, respectively, are given by equations (6) and (7) [*Šimůnek et al*., 2012].

$$K_{SP}^G=\left(Ca^{2+}\right)\left(SO_4^{2-}\right)(H_2O)^2, \tag{6}$$

$$K_{SP}^C=\left(Ca^{2+}\right)\left(CO_3^{2-}\right). \tag{7}$$

where parentheses represent ion activities. A more thorough explanation can be found in *Suarez and Šimůnek* [1997] and *Šimůnek et al*. [2012].

Numerical solution of the Richards equation, which describes water flow in soils, requires the knowledge of soil hydraulic functions that relate the pressure head, the water content, and the hydraulic conductivity of the soil. Soil hydraulic parameters required for the water flow model when the van Genuchten-Mualem model [*van Genuchten*, 1980] is used are the residual water content, θ_r [$L^3\,L^{-3}$], the saturated water content, θ_s [$L^3\,L^{-3}$], and the shape parameters α [L^{-1}], and n for the soil water retention function, and the saturated hydraulic conductivity K_s [$L\,T^{-1}$], and the tortuosity factor l for the hydraulic conductivity function.

4. Parameterization of HYDRUS (2D/3D) and Its UNSATCHEM Module

The HYDRUS-1D and HYDRUS (2D/3D) software packages [*Šimůnek et al*., 2008] were used to inversely estimate selected transport and reaction parameters using different techniques. As stated previously, parameterization processes can highly influence the quality and relevance of modeled results. Each calibration step was performed at a specific dimension (1-D or 3-D) and with a different optimization tool while taking into

Table 2. Soil Texture, Hydraulic and Transport Parameters and Exchange Coefficients of the Loamy Sand Soil[a]

Soil Parameter	Units	Value	S.E. Coefficient
θ_r	($cm^3\ cm^{-3}$)	0.004	
θ_s	($cm^3\ cm^{-3}$)	0.36	0.007
α	(cm^{-1})	0.016	0.0006
n		3.43	0.36
l		0.5	
K_S	($cm\ d^{-1}$)	145.44	
ρ_b	($g\ cm^{-3}$)	1.5	
Sand	(%)	89	
Clay	(%)	4	
Silt	(%)	7	
K_G (Mg/Ca)		0.43	0.08
K_G (Ca/Na)	($L\ meq^{-0.5}$)	0.14	0.04
K_G (Ca/K)	($L\ meq^{-0.5}$)	0.60	0.1
CEC	($meq\ kg^{-1}$)	43.7	
λ_L	(cm)	1.7	
λ_T	(cm)	0.17	

[a]θ_r, residual water content; θ_s, saturated water content; α and n, empirical shape parameters; l, tortuosity factor; K_S, saturated hydraulic conductivity; ρ_b, bulk density, K_G, Gapon exchange coefficients for different cation pairs; *CEC*, cation exchange capacity; λ_L and λ_T, longitudinal and transverse dispersivities, respectively.

consideration the computational times and the scale/dimension dependency of each parameter to be calibrated.

Hydraulic parameters of the loamy sand soil were either estimated using the RETC software [*van Genuchten et al*., 1991] or measured in the laboratory. The dispersivities, which are highly scale-dependent [*Neuman*, 1990; *Vanderborght and Vereecken*, 2007], were manually calibrated using HYDRUS (2D/3D) in three-dimensional simulations. The dimension-independent Gapon exchange coefficients were optimized using the external software UCODE and HYDRUS-1D. HYDRUS-1D was used rather than HYDRUS (2D/3D) because of high computational requirements when running three-dimensional simulations. Finally, the initial adsorbed and precipitated concentrations were estimated by trial and error.

Optimized parameters using either RETC, UCODE, or HYDRUS were obtained by minimizing the objective function defined as the sum of weighted least squares. This function compares each observed data point to the corresponding modeled value

$$S(\boldsymbol{b}) = \sum_{i=1}^{n} \omega_i [y_i - y'_i(\boldsymbol{b})]^2, \tag{8}$$

where $S(\boldsymbol{b})$ is the objective function, $\boldsymbol{b}$ is a vector of optimized parameters, n is the number of data points, ω_i is the weight associated with each data point, y_i is the observed data point, and $y'_i(\boldsymbol{b})$ is the data point calculated using the parameters $\boldsymbol{b}$.

Constant weights were used in the RETC and HYDRUS (2D/3D) optimizations. In the UCODE optimization, the coefficients of variation, calculated as the ratio between the averaged and standard deviations of the four replications, were used as weights.

4.1. Soil Hydraulic Parameters

The θ_s, α, and n parameters of the van Genuchten-Mualem hydraulic model [*van Genuchten*, 1980] were estimated using the RETC computer program [*van Genuchten et al*., 1991] (Table 2). Water contents at 16 depths under hydrostatic conditions from the 0.85 m long column and water contents at pressure heads of −5 and −8 m were used as input data for the objective function of the optimization. The saturated hydraulic conductivity, K_S, was determined using the constant head method [*Ali*, 2010] in 20 cm long backfilled soil columns with a diameter of 5 cm. The residual water content, θ_r, was assumed to be equal to the measured soil water content at a soil water pressure head of −8 m. Bulk density, ρ_b, was measured using undisturbed soil core samples. The shape parameter l was assumed to be 0.5 as used before for similar soils [*Ityel et al*., 2011]. The θ_r, K_S, and l parameters were used as prior information for the inverse problem. A summary of the hydraulic properties and their related statistics can be found in Table 2.

4.2. Gapon Exchange Parameters

Gapon exchange parameters can be calculated from measured values of soluble and exchangeable concentrations using equation (3) [*Gonçalves et al*., 2006; *Ramos et al*., 2011]. However, since some of these concentrations are relatively low, small measurement errors can have a great influence on calculated values [*Smiles and Smith*, 2004]. The Gapon exchange coefficients can also be estimated from a predefined range of known values for a specific soil [*MDH Engineered Solutions Corp*., 2003; *Šimůnek et al*., 2012] or inversely estimated from measured soil solution and adsorbed concentrations [*Jacques et al*., 2012]. Here the Gapon

Table 3. Initial Adsorbed and Precipitated Concentrations for the 1-D and 3-D Simulations

Adsorbed Concentrations (meq kg^{-1})				Precipitated Concentrations (meq kg^{-1})	
Ca^{2+}	Mg^{2+}	Na^{+}	K^{+}	Calcite	Gypsum
8.7	20	14	1	3197	27 (1-D)/22 (3-D)

coefficients were estimated using the general optimization code UCODE_2014 [*Poeter et al*., 2005, 2014] and HYDRUS-1D coupled with UNSATCHEM. As shown in *Poeter et al*. [2014], UCODE can be used to inversely estimate parameters that cannot be estimated using the built-in inverse module in HYDRUS-1D. The observation data were obtained by averaging the drainage solute concentrations from the four shallow lysimeters. Five different solute concentrations (Na^{+}, Ca^{2+}, Mg^{2+}, K^{+}, and SO_4^{2-}), and EC values measured in the drainage solution at 19 different time points, resulted in a total of 114 data points. Modeled concentrations obtained at an observation point located at the lower boundary of a 1-D profile were fitted against the measured drainage concentrations data. This approach assumes that the resident concentration at the observation point in the seepage face equals the modeled drainage concentration. Estimated values of the Gapon coefficients and associated statistics are given in Table 2.

Adsorbed Ca^{2+}, Mg^{2+}, Na^{+}, and K^{+}, as well as precipitated calcite and gypsum, concentrations were measured in soil samples obtained in the same area as the soil used for the experiment and were used as a starting point for the simulations. They were all, except for the calcite concentrations, changed as needed in order to match the first drainage concentration measurement by the model (Table 3). This exercise was performed in 1-D due to its shorter computational times, the relative scale independence of exchange coefficients and the assumption of homogeneous adsorbed and precipitated initial concentrations along the lysimeter profile. The 1-D profile had a depth of 0.25 m and a LBC defined as a seepage face with a pressure head of −30 cm. Initial pressure heads and soil solution concentrations were uniform along the profile with values of −100 cm and the solution composition of GW (Table 1), respectively.

4.3. Longitudinal and Transverse Dispersivities

Longitudinal dispersivity (λ_L) for the deep lysimeters was optimized in 3-D by manually finding the level within a range between 0.5 and 5 cm best fitting measured results. The transverse dispersivity (λ_T) was maintained at one tenth of the λ_L as suggested in the literature [*Bear*, 1972; *Skaggs and Leij*, 2002; *Šimůnek and van Genuchten*, 2006]. Results from a total of 17 simulations were compared to observed data and the objective function was calculated according to equation (8). A total of 56 data points were included in the objective function comparing modeled and measured chloride concentrations of drainage solution at 38 times and 18 resident concentrations representing suction cup solution. In coarse soils, resident concentrations can be used to represent pore water solutions [*Jacobsen et al*., 1992]. The lowest objective function value, as defined in equation (8), was found for $\lambda_L = 1.7$ cm and $\lambda_T = 0.17$ cm (Figure 2). Such manual calibration enabled a less tedious optimization in 3-D because the transverse dispersivity was a function of the longitudinal dispersivity, eliminating the need to determine them separately.

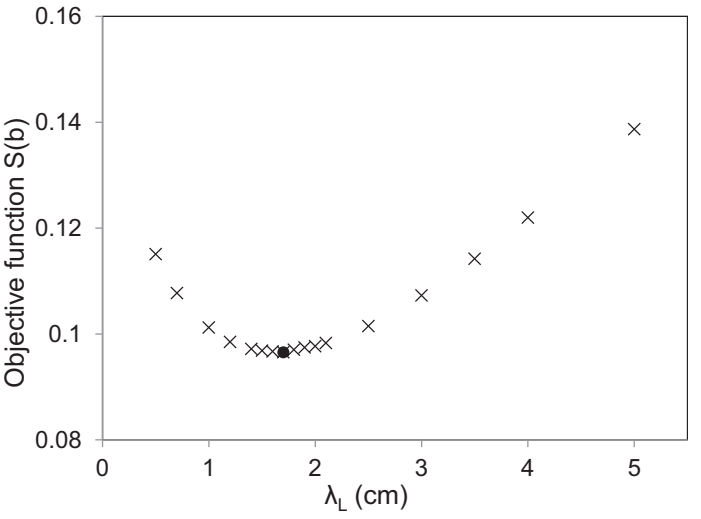

Figure 2. Objective function as a function of dispersivity. The black dot represents the minimum of the objective function.

5. Modeling Three-Dimensional Multicomponent Solute Transport

Optimized transport and exchange parameters were used to model the three-dimensional water flow

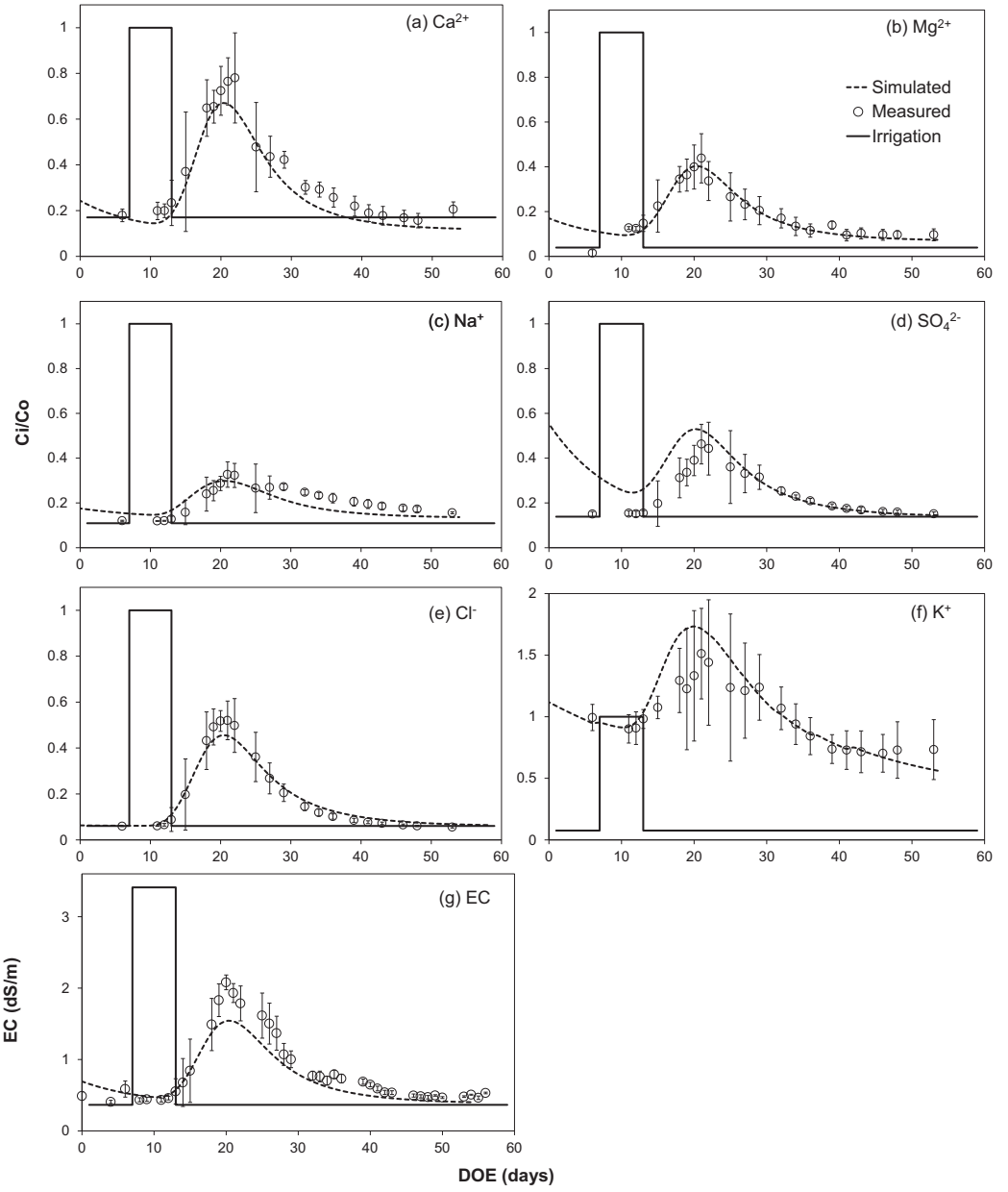

Figure 3. Simulated (dashed lines) and measured (symbols) relative concentrations of major ions in the drainage water. Error bars represent one standard deviation. DOE stands for day of experiment.

and multicomponent solute transport in the lysimeter experiment. The three-dimensional transport domain had surface dimensions of 0.35 and 0.7 m and a depth of 0.5 m (Figure 1). An observation point was defined in the center of the lysimeter at a depth of 0.25 m, at the location of the soil pore water suction device (Figure 1). Twenty horizontal equally spaced planes were discretized using an unstructured finite element mesh, resulting in a total of 14,640 nodes and 26,068 three-dimensional tetrahedral elements (Figure 1).

The initial condition for water flow was defined as hydrostatic equilibrium with a pressure head of −30 cm at the bottom of the soil profile. The initial soil solution was assumed to have the same solute concentrations as the GW because the field, from which the soil was obtained, was previously irrigated with that water quality. Adsorbed and precipitated concentrations were the same as in 1-D simulations, except for the gypsum concentrations, which had to be reduced to 22 meq kg^{-1} in the 3-D domain where its leaching is not as effective as in 1-D. The initial CO_2 concentration was assumed to be equal to average atmospheric values (400 ppm) [*NOAA-ESRL*, 2015].

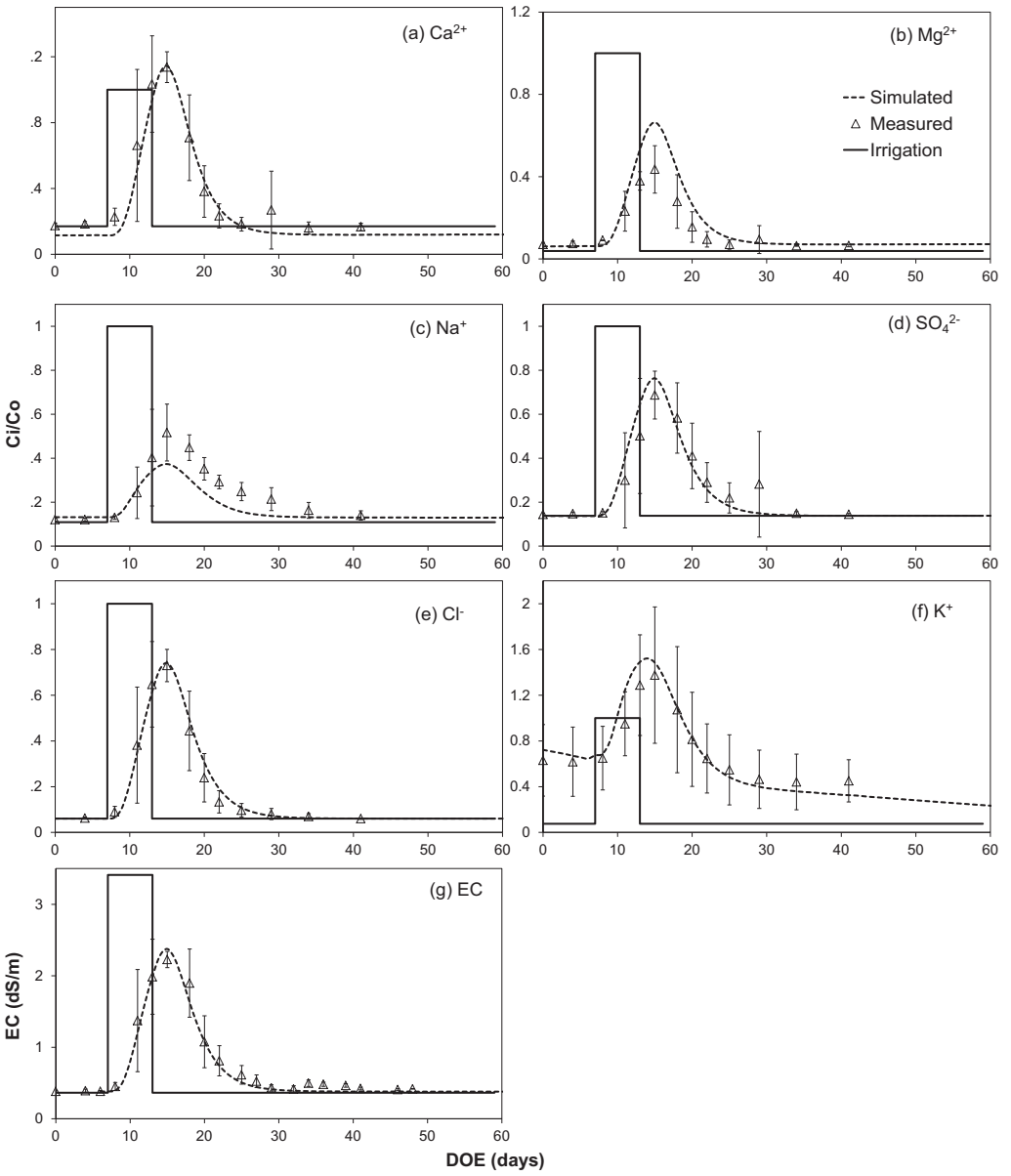

Figure 4. Simulated (dashed lines) and measured (symbols) relative concentrations of major ions in the soil solution collected using ceramic suction devices. Error bars represent one standard deviation. DOE stands for day of experiment.

The upper BC was defined as no flow, except for four separate areas of 2.4 cm^2 each representing drippers, in which a variable flux BC with specified solute concentrations was assigned. Two liters of water per day of varying quality were applied during the entire simulation as in the actual experiment. The flushing period with DW (first 60 days) water is not shown in the results and the day of experiment (DOE) begins 6 days before the pulse with GW starts. The lower boundary was defined as no flow, except for two circles, representing the outflow drainage extensions, for which a seepage face BC with the pressure head of −30 cm was specified (Figure 1). This pressure head at the lower BC was an average of measurements in lysimeters with the same LBCs. All remaining boundaries were defined as no-flow boundaries (Figure 1). A third type, Cauchy BC, was used for solute transport at both the upper and lower boundaries.

5.1. Calibration Results

Measured and simulated relative major ion concentrations are presented in Figures 3 and 4. Relative concentrations were calculated by dividing the actual concentration of a particular ion by its concentration in

Table 4. Correlations Between Modeled and Measured Data[a]

	$[Ca^{2+}]$	$[Mg^{2+}]$	$[Na^{+}]$	$[K^{+}]$	$[SO_4^{2-}]$	$[Cl^{-}]$	All Solutes	EC
Drainage								
R^2	0.96	0.92	0.63	0.70	0.69	0.98	0.94	0.94
Slope	1.13	0.99	1.04	0.89	0.79	1.07	0.91	1.20
N	22	22	22	22	22	22	132	40
r	0.99	0.96	0.81	0.95	0.86	1.00	0.92	0.97
Soil Water Solution								
R^2	0.95	0.95	0.87	0.90	0.86	0.98	0.93	0.97
Slope	1.04	0.68	1.28	0.92	0.94	0.98	0.95	1.03
N	13	13	13	13	13	12	77	20
r	0.98	0.99	0.93	0.98	0.95	0.99	0.94	0.99
All Samples								
R^2	0.95	0.83	0.74	0.83	0.78	0.97	0.94	0.94
Slope	1.09	0.84	1.14	0.89	0.85	1.02	0.92	0.87
N	35	35	35	35	35	34	209	60
r	0.98	0.93	0.86	0.96	0.90	0.96	0.93	0.97

[a]Data for soil water and drainage solution concentrations from the rotating lysimeter system experiment. Measured EC (electrical conductivity) was compared to simulated EC calculated from cations.

the brackish water (GW in Table 1). Both figures also show the timing of the period of saline irrigation water application and the error bars associated with the concentration measurements in the four lysimeters. Simulated and averaged measured data were compared using linear regression with an intercept equal to zero. Numbers of observations, slopes, coefficients of determination (R^2), and correlation coefficients (r) are shown in Table 4. Regressions were performed for each ion, all solutes together, and the measured EC as a function of the EC calculated from simulated cations (as in *Bresler et al.* [1982]).

The modeled drainage concentrations of Ca^{2+}, Mg^{+}, and Cl^{-} were in good agreement with the measured concentrations (Figure 3 and Table 4). The modeled concentrations of sodium were over and underestimated at the beginning and end of the pulse of saline water, respectively. However, the peak relative values of sodium were well predicted by the model. Sulfate drainage concentrations were lower than those predicted by the model at the beginning of the experiment. Potassium modeled drainage concentrations were in the range of one standard deviation from the average measured values.

The modeled soil solution concentrations of Ca^{2+}, SO_4^{2-}, Cl^{-}, and K^{+} were in good agreement with the measured concentrations (Figure 4 and Table 4). Measured sodium concentrations of the soil solution samples were higher than the modeled concentrations during the breakthrough of saline water. Magnesium soil solution concentrations were underestimated by the model (slope = 0.68). However, the overall trend of measured concentrations is described well as indicated by a high coefficient of determination ($R^2 = 0.93$) and a slope value close to one (0.95). Measured relative concentrations of potassium were characterized by high variability and values higher than one for both the drainage and soil solution relative concentrations. This is probably due to the failure to completely leach potassium before applying the saline water and a possible presence of different initial amounts of potassium in the soil of each lysimeter.

Overall salinity, evaluated using simulated cations (as in *Bresler et al.* [1982]), was comparable to measured *EC*. The values presented in Figure 3g for the drainage solutions and Figure 4g for the soil water solutions showed good agreement between the simulated and measured data with an R^2 of 0.94 and a slope of 0.87 (60 samples, Table 4).

The effect of uncertainty and variability in Gapon coefficient values on the results was studied with a sensitivity analysis in the range of the 95% confidence interval for the optimized Gapon coefficients (Supporting Information). It was found that the variability caused by using different Gapon coefficients was similar to the variability of the measured data.

6. Lysimeter Design Evaluation

A hypothetical example was analyzed, in which a crop was grown in a lysimeter with the same dimensions as in the rotating lysimeter system while three different seepage face values, situated at the same location as in Figure 1, were considered. Simulation time was selected so that transient drainage concentrations and

Table 5. Root Water Uptake Parameters for the Hypothetical Example

Water Stress Response Function Parameters		
P50	cm	−800
P3		3
PW	cm	−1.00E+10
Salinity Stress Response Function Parameters		
c50	cm	−2417
P3		1.65
Osmotic coefficient		1

leaching fractions reached steady state. The seepage face BCs were considered with pressure head values of 0, −30, and −100 cm. The first case represented a scenario in which a free-drainage lysimeter has no drainage extensions and no suction devices [e.g., *Flury et al*., 1999; *Abdou and Flury*, 2004; *Gonçalves et al*., 2006]. This lower boundary condition is the one generally applied to containers used in nurseries and in detached growing media. In the second case, the pressure head was the same as during the actual experiment, representing a lysimeter with highly conductive drainage extensions. In the third case, the pressure head of −100 cm represented a scenario in which the bottom suction is applied using suction plates or similar devices [e.g., *Evett et al*., 2012; *Skaggs et al*., 2012]. This range of LBCs is applicable not only to lysimeters but to crop experiments performed in pots, or to horticulture implemented in detached soilless media with limited root zone volume [e.g., *Ben-Gal et al*., 2009; *Shenker et al*., 2011; *Caron et al*., 2015b].

Irrigation (I) was applied continuously through four drippers at a rate of 1.1 L/d (representing 4.5 mm/d according to the lysimeter area) with the solution composition defined as GW in Table 1. Potential transpiration (T_p) was 3 mm/d and evaporation was neglected, so that the ratio of I/T_p was 1.5. The initial pressure head was set to −30 cm at the bottom of the lysimeter and −80 cm at the soil surface, with a linear interpolation between these two depths. The initial soil solution concentrations were set as equal to the irrigation water quality. The initial adsorbed and precipitated concentrations were the same as the ones used in the previous 3-D simulation.

Contrary to the experiment, in which there were no plants present, root water uptake was considered in the hypothetical scenarios. The vertical root distribution was defined according to the model of *Vrugt et al*. [2001] with the following parameters: a maximum rooting depth of 30 cm, a depth of maximum intensity of 20 cm, and a shape parameter *Pz* of 2. S-shaped stress response functions were used for both water and osmotic stresses, the effect of which was assumed to be multiplicative [*van Genuchten*, 1987]. Parameters defining the S-shaped water uptake reduction functions for water and osmotic stresses are defined in Table 5 as calculated in *Groenveld et al*. [2013] for similar conditions. Compensated root water uptake was considered by setting the critical stress index to 0.5 [*Šimůnek and Hopmans*, 2009].

Leaching fractions were calculated daily and independently for water fluxes (LF_w), chloride concentrations (LF_{Cl-}), and EC (LF_{EC}) for each simulation according to [*Ayers and Westcot*, 1994]

$$LF_w = \frac{D}{I}, \tag{9a}$$

$$LF_{Cl^-} = \frac{[Cl^-]_I}{[Cl^-]_D}, \tag{9b}$$

$$LF_{EC} = \frac{EC_I}{EC_D}. \tag{9c}$$

Exchangable sodium percentage (ESP) was calculated as the percentage of adsorbed sodium from the total CEC (Table 2), which was assumed to be constatnt through the simulations. The ESP spatial profiles were compared at four different times (50, 100, 150, and 200 days). The results are presented for a cross sectional area at the dripper location X = 20.26 cm.

6.1. Effects of the Lysimeter Design on the Transient Leaching Fraction and ESP Profile Distribution

Relative drainage concentrations for various solutes are presented in Figure 5 for three different lysimeter designs. With a pressure head of 0 cm at the seepage face there was no drainage during the first 29 days. As expected, the lower the pressure head at the seepage face, the earlier the concentration peak due to the leaching of dissolved solutes from adsorbed and precipitated species. The drainage concentrations for the three different LBCs during the season show the dynamic effects of solute leaching as a result of solute

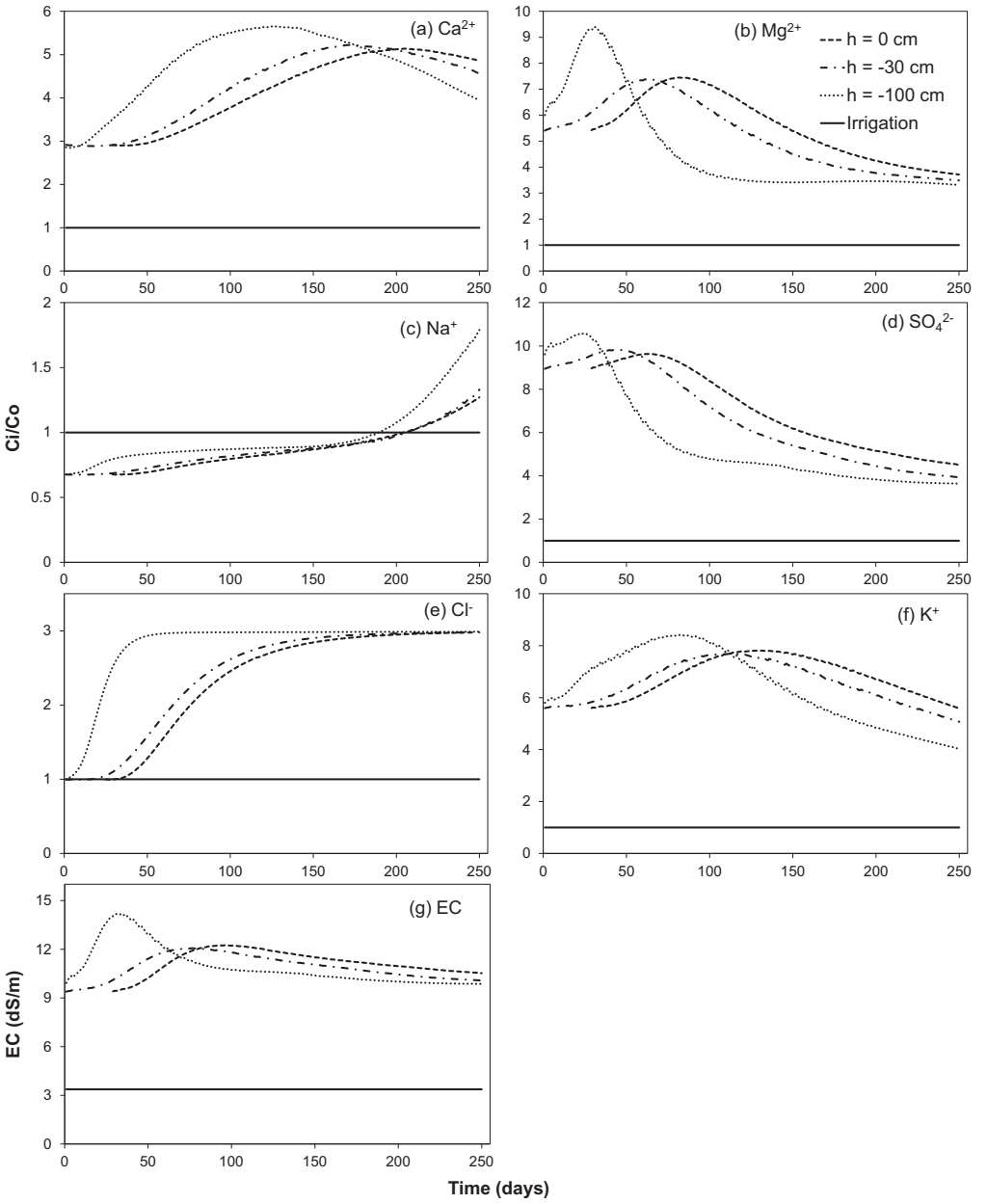

Figure 5. Simulated relative major ion concentrations and EC in the drainage water for three different lysimeter designs represented by a seepage face bottom BC with pressure heads (h) of 0, −30, and −100 cm.

precipitation, adsorption and dissolution processes. An impact of these processes is visible in the increase of Na^+ concentrations in drainage after day 190 and the simultaneous decrease of Ca^{2+} concentrations.

Since a constant theoretical leaching fraction of 0.33 was set according to applied irrigation and potential transpiration rates, it was expected that steady state would be reached for both water and solutes (Figure 6) [*Letey et al.*, 2011; *Tripler et al.*, 2012]. Steady state was assumed when each leaching fraction reached a value of 99% of the final corresponding leaching fraction. Initial LF_{Cl} were high due to relative lower Cl^- concentrations at the beginning of the simulation and subsequent accumulation during the growing season until steady state was achieved. Initial LF_{EC} were lower than those of the LF_{Cl} due to a combination of solute leaching at the beginning of the simulation (mainly SO_4^{2-} from gypsum dissolution, Figure 5) and subsequent solute accumulation with time. Identical steady state values were achieved for all lysimeters for LF_W and LF_{Cl} (Table 6), except for the LF_{Cl} for the −100 cm seepage face lysimeter. The lower the seepage face pressure head, the higher the steady state value for LF_{EC} (Table 6). Initial LF_{EC} values were almost identical for all treatments. However, these

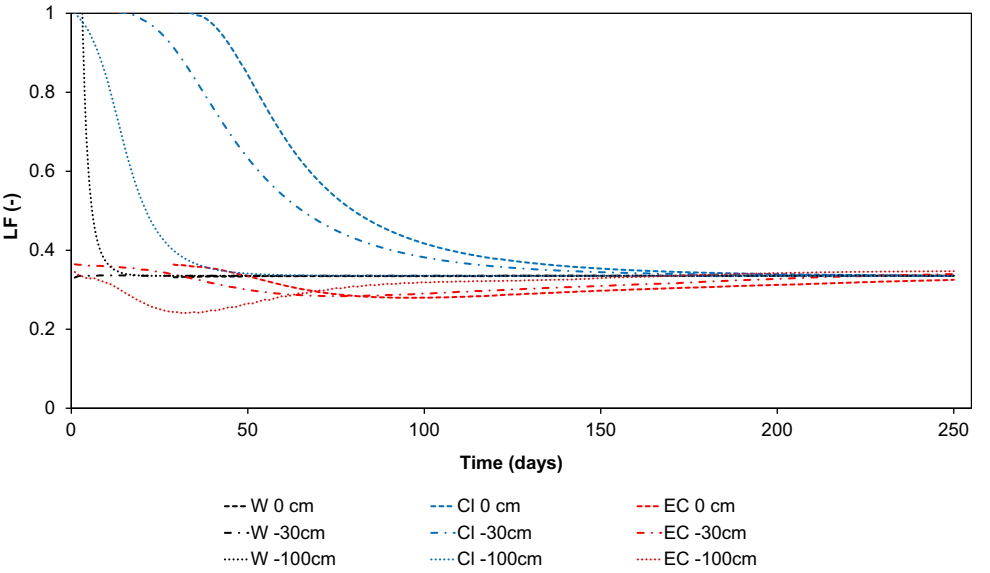

Figure 6. Simulated leaching fractions (LF) calculated from water fluxes (black), chloride concentrations (blue), and EC values (red) according to equation (9).

values changed with the progress of the simulation. This was due to a combination of higher water content in the root zone, higher pore water velocity, and its effect on cation exchange and precipitation/dissolution processes that affect calculated EC. Higher pore water velocities result in higher hydrodynamic dispersion, therefore causing LF_{Cl} and LF_{EC} to achieve steady state earlier for lysimeters with lower seepage face pressure heads (Table 6 and Figure 6). LF_W reached steady state already during the first day of flow for the simulations with the 0 and −30 cm seepage face BCs (day 29 is the first day of outflow for the 0 cm lysimeter), while it took 16 days for the simulation with the −100 cm seepage face BC to reach steady state. This is due to the relative difference between the initial pressure head distribution along the profile, which was identical for all simulations (hydrostatic equilibrium with a pressure head of −30 cm at the bottom of the soil profile), and the final steady state distributions, which were different, reflecting the different lysimeter designs. The lysimeter with the seepage face BC value of −30 cm had a pressure head profile distribution at steady state very similar to the imposed initial condition, reaching steady state for the LF_W already at the first day of the simulation.

There has been wide interest in the concept of the leaching fraction and whether it should be evaluated using transient or steady state models [*Corwin et al.*, 2007; *Letey and Feng*, 2007; *Dudley et al.*, 2008b; *Letey et al.*, 2011]. By considering the complex multidimensionality of flow and transport patterns in lysimeters resulting from imposed BCs (e.g., drippers and drainage outlet designs), the modeling approach presented in this paper offers an opportunity for a better understanding of how the spatial distributions of water contents, water fluxes, and dissolved, precipitated, and adsorbed solute concentrations influence measured leaching fractions. The model showed that, in the long term, after the system reaches steady state conditions, there was no effect on LF_W and LF_{Cl}. However, different LBCs did affect salt distribution in the profile and the steady state LF_{EC} values. If transient response, and not only steady state conditions, is of interest, the effects of the different drainage outlet designs are expected to become even more relevant.

ESP values in the simulated profiles for different LBCs ranged between 10 and 30 and decreased with time (Figure 7). Differences in ESP values between the simulations at the same time step were as high as 8, with the largest variations found comparing seepage face pressure head values of 0 and −100 cm. The largest

Table 6. Values of the Leaching Fraction at Steady State and Simulation Time When Steady State Was Reached

	Days to Steady State			LF Values at Steady State		
Seepage Face Pressure Head	LF_W	LF_{Cl}	LF_{EC}	LF_W	LF_{Cl}	LF_{EC}
0 cm	29	192	229	0.34	0.34	0.33
−30 cm	1	169	225	0.34	0.34	0.34
−100 cm	16	53	198	0.34	0.33	0.35

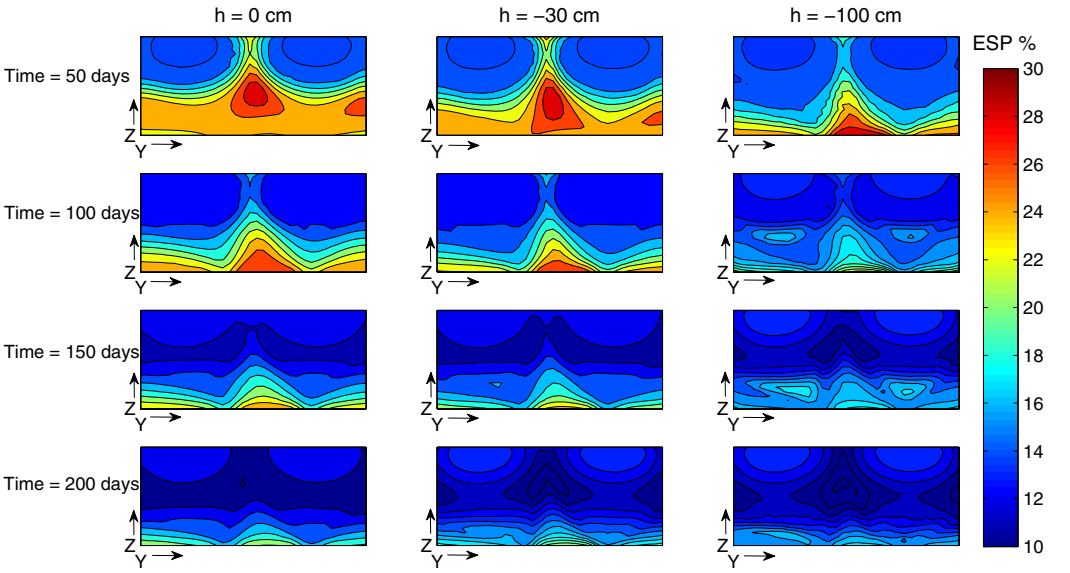

Figure 7. Exchangeable sodium percentage (ESP) spatial distributions for simulations with seepage face values of 0, −30, and −100 cm at four times in a cross section 50 cm wide (Z) and 70 cm high (Y) at X = 20.26 cm (see Figure 1).

discrepancies in ESP were consistently located below the root zone, close to the LBC. It is well known that increased ESP may influence hydraulic conductivity [*McNeal and Coleman*, 1966; *McNeal*, 1968; *Frenkel et al*., 1978; *Shainberg et al*., 1980; *Crescimanno et al*., 1995] depending on the soil type, water quality, and pH [*Šimůnek et al*., 2012]. Varying ESP values within a lysimeter profile could affect local hydraulic conductivities, leading to altered water flow and solute transport patterns. If studies of reclamation of sodic soils or irrigation with varying water qualities are to be assessed using lysimeters, then understanding the adsorbed and dissolved solute distributions throughout the lysimeter profile becomes critical.

Different salinities and water contents due to different BCs could also affect root water uptake, depending on the uptake and stress parameters related to particular crops. Soilless media used for food production in containers or constructed root zones using imported media in the soil itself introduce salts that may necessitate leaching before plant establishment or during the growing season. While water flow in various growing media has been studied and characterized [*Raviv and Lieth*, 2008; *Caron et al*., 2015b], there are still knowledge gaps concerning solute transport, exchange processes and nutrient availability in detached, or otherwise imported, growing systems designed to increase crop production [*Heinen*, 2001; *Ityel et al*., 2011; *Caron et al*., 2015a]. Salinity in specific areas of the root zone, produced by a combination of irrigation water quality, delivery method, discharge rate, evaporative demand, and container or root zone medium geometry and size can limit root growth and therefore plant development [*Raviv and Lieth*, 2008]. The calibrated model presented in this study can be used in order to compare the solute distribution in containers or constructed root zones of different sizes and with different irrigation strategies, as well as their differences with the distributions expected under more traditional field conditions. The approach of the current study could prove beneficial to other cases necessitating three-dimensional consideration, for example, drip irrigation of particularly variable soils, orchards irrigated with low-quality waters [*Russo et al*., 2013], as a method to evaluate solute transport as affected by root zone profile depth due to presence of a shallow water table or impermeable soil horizon.

In addition, the model can be used to study the differences between conditions produced in artificial root zones including lysimeters or growing containers, and parallel field conditions and to analyze design and management criteria of the constructed root zones, particularly with respect to the choice of geometry, the bottom BC, and dripper location and discharge rate. Once the design criteria are chosen, the model can be further applied in order to assess different methods of transient *LF* calculations for prediction of salinity management.

7. Conclusions

HYDRUS (2D/3D) coupled with UNSATCHEM was successfully applied to simulate and describe three-dimensional transient water flow and multicomponent solute transport in lysimeters. Monitored

concentrations in drainage and soil pore water solutions from lysimeter experiments, in which variable water qualities were used for irrigation, correlated well with simulated values, with $R^2 = 0.94$ and a slope of 0.92 for all solutes measured in the drainage and soil solution samples ($n = 209$). For 60 pairs of measured and modeled EC values, R^2 was 0.94 with a slope of 0.87. Models with specific chemistry, such as UNSATCHEM coupled with HYDRUS (2D/3D), are less flexible than general geochemical models [*Šimůnek et al*., 2014], but they are simpler to use and implement. In addition, it should be noted that long computational times are required for multicomponent multidimensional modeling, and it may be advantageous to streamline the system by using simpler geometries and models of lower dimension (3-D/2-D/1-D).

While active and passive root solute uptake are included in the standard HYDRUS (2D/3D) [*Šimůnek et al*., 2016], solute uptake is not considered when the multicomponent solute transport module is activated [*Šimůnek et al*., 2012]. Considering specific solute uptake could help describe processes such as ion toxicity and subsequent water uptake reductions. Solute uptake could also be important in quantifying moderate changes in the soil solution composition, especially for irrigation with varying water qualities [*Groenveld et al*., 2013; *Silber et al*., 2015]. Combining multicomponent root uptake models, such as the one presented by *Silberbush and Ben-Asher* [2001], in soil-based models such as HYDRUS (2D/3D), could improve simulations of cropping systems [*Schröder et al*., 2012; *Raij et al*., 2013].

The calibrated model was used to study the effects of lysimeter design on transient leaching fractions and on ESP profile distribution. Different lysimeter outlet designs led to slightly different steady state leaching fractions calculated using EC. Transient responses of the LFs between initial conditions and steady state were a function of the LBC. Disparities in profile ESP were found as a function of lysimeter design, demonstrating the potential of the calibrated model for studying how LBCs affect the profile chemistry and its consequence on hydraulic conductivity.

As discussed by *Šimůnek et al*. [2016], HYDRUS has been widely used for simulating soil water, solute and nutrient distribution for different drip irrigation with varying levels of salinity. However, the past studies were either one-dimensional [*Gonçalves et al*., 2006; *Ramos et al*., 2011] or considered only a single solute or general salinity as a tracer [*Ajdary et al*., 2007; *Ramos et al*., 2012; *El-Nesr et al*., 2013]. When using drip irrigation with water containing salts, ions are leached from the root zone to the surrounding areas, generating favorable conditions for plant roots [*Hanson et al*., 2009; *Phogat et al*., 2012; *Shan and Wang*, 2012; *Chen et al*., 2014; *Mguidiche et al*., 2015]. This process can be modeled in a 2-D axisymmetrical domain as long as the wetted areas of each dripper do not overlap [*Kandelous et al*., 2011]. The model presented in this study can describe water flow and solute movement in a complex three-dimensional root zone, where water contents and dissolved, adsorbed and precipitated species are highly variable. HYDRUS (2D/3D) coupled with UNSATCHEM can be used to analyze and optimize design of field lysimeters for in situ monitoring of solute leaching, for prevention of soil salinization, and for monitoring of salts and agrochemicals moving out of the root zone and into deep soils and groundwater. In addition, the model can assist in designing lysimeters, commercial growing containers or constructed root zones for better management of irrigation with low-quality waters, providing information concerning spatial distribution of general salinity, specific solute ions, and adsorbed and precipitated species.

Acknowledgments

This research was partially supported by the Israel Ministry of Agriculture and Rural Development (Eugene Kandel Knowledge centers) as part of the Root of the Matter - The root zone knowledge center for leveraging modern agriculture, I-CORE Program of the Planning and Budgeting Committee and The Israel Science Foundation (grant 152/11), by the Goldinger Trust and the USDA ISE Program (grant 2010-51160-21070). The data of this paper are available upon request (iael@post.bgu.ac.il).

References

Abdou, H. M., and M. Flury (2004), Simulation of water flow and solute transport in free-drainage lysimeters and field soils with heterogeneous structures, *Eur. J. Soil Sci.*, *55*(2), 229–241, doi:10.1046/j.1365-2389.2004.00592.x.

Ajdary, K., D. K. Singh, A. K. Singh, and M. Khanna (2007), Modelling of nitrogen leaching from experimental onion field under drip fertigation, *Agric. Water Manage.*, *89*, 15–28, doi:10.1016/j.agwat.2006.12.014.

Ali, M. H. (2010), *Fundamentals of Irrigation and On-Farm Water Management*, vol. 1, Springer, N. Y.

Allen, R. G., L. S. Pereira, D. Raes, and M. Smith (1998), *Crop Evapotranspiration: Guidelines for Computing Crop Water Requirements, FAO Irrig. Drain*. Pap. 56, Food and Agric. Organ. of the U. N., Rome.

Ayers, R. S., and D. W. Westcot (1994), *Water Quality for Agriculture*, *FAO Irrig. Drain. Pap. 29*, Food and Agric. Organ. of the U. N., Rome.

Bear, J. (1972), *Dynamics of Fluids in Porous Media*, Am. Elsevier Publ. Co., N. Y.

Ben-Gal, A., and U. Shani (2002), A highly conductive drainage extension to control the lower boundary condition of lysimeters, *Plant Soil*, *239*, 9–17.

Ben-Gal, A., H. Borochov-Neori, U. Yermiyahu, and U. Shani (2009), Is osmotic potential a more appropriate property than electrical conductivity for evaluating whole-plant response to salinity?, *Environ. Exp. Bot.*, *65*, 232–237, doi:10.1016/j.envexpbot.2008.09.006.

Bergström, L. (1990), Use of lysimeters to estimate leaching of pesticides in agricultural soils, *Environ. Pollut.*, *67*(4), 325–347.

Bhantana, P., and N. Lazarovitch (2010), Evapotranspiration, crop coefficient and growth of two young pomegranate (*Punica granatum* L.) varieties under salt stress, *Agric. Water Manage.*, *97*(5), 715–722, doi:10.1016/j.agwat.2009.12.016.

Bresler, E., B. L. McNeal, and D. L. Carter (1982), *Saline and Sodic Soils*, edited by D. F. R. Bommer, et al. Springer, Berlin.
Bryla, D. R., T. J. Trout, F. Collins, and J. E. Ayars (2010), Weighing lysimeters for developing crop coefficients and efficient irrigation practices for vegetable crops, *HortScience*, *45*(11), 1597–1604.
Caron, J., R. Heinse, and S. Charpentier (2015a), Organic materials used in agriculture, horticulture, reconstructed soils, and filtering applications, *Vadose Zone J.*, *14*(6), 1–6, doi:10.2136/vzj2015.04.0057.
Caron, J., J. S. Price, and L. Rochefort (2015b), Physical properties of organic soil: Adapting mineral soil concepts to horticultural growing media and histosol characterization, *Vadose Zone J.*, *14*(6), 1–14, doi:10.2136/vzj2014.10.0146.
Chen, L. J., Q. Feng, F. R. Li, and C. S. Li (2014), A bidirectional model for simulating soil water flow and salt transport under mulched drip irrigation with saline water, *Agric. Water Manage.*, *146*, 24–33, doi:10.1016/j.agwat.2014.07.021.
Chen, W., Z. Hou, L. Wu, Y. Liang, and C. Wei (2010), Evaluating salinity distribution in soil irrigated with saline water in arid regions of northwest China, *Agric. Water Manage.*, *97*, 2001–2008, doi:10.1016/j.agwat.2010.03.008.
Corwin, D. L. (2002), Miscible solute transport: Suction cups, in *Methods of Soil Analysis, Part 4: Physical Methods*, edited by J. H. Dane and G. C. Topp, pp. 1261–1266, Soil Sci. Soc. of Am., Madison, Wis.
Corwin, D. L., J. D. Rhoades, and J. Šimůnek (2007), Leaching requirement for soil salinity control: Steady-state versus transient models, *Agric. Water Manage.*, *90*(3), 165–180, doi:10.1016/j.agwat.2007.02.007.
Crescimanno, G., M. Iovino, and G. Provenzano (1995), Influence of salinity and sodicity on soil structural and hydraulic characteristics, *Soil Sci. Soc. Am. J.*, *59*, 1701–1708, doi:10.2136/sssaj1995.03615995005900060028x.
Dudley, L. M., A. Ben-Gal, and N. Lazarovitch (2008a), Drainage water reuse: Biological, physical, and technological considerations for system management, *J. Environ. Qual.*, *37*, S25–S35, doi:10.2134/jeq2007.0314.
Dudley, L. M., A. Ben-Gal, and U. Shani (2008b), Influence of plant, soil, and water on the leaching fraction, *Vadose Zone J.*, *7*, 420–425, doi:10.2136/vzj2007.0103.
El-Nesr, M. N., A. A. Alazba, and J. Šimůnek (2013), HYDRUS simulations of the effects of dual-drip subsurface irrigation and a physical barrier on water movement and solute transport in soils, *Irrig. Sci.*, *32*(2), 111–125, doi:10.1007/s00271-013-0417-x.
Evett, S. R., R. C. Schwartz, T. A. Howell, R. L. Baumhardt, and K. S. Copeland (2012), Can weighing lysimeter ET represent surrounding field ET well enough to test flux station measurements of daily and sub-daily ET?, *Adv. Water Resour.*, *50*, 79–90, doi:10.1016/j.advwatres.2012.07.023.
Flury, M., M. V. Yates, and W. A. Jury (1999), Numerical analysis of the effect of the lower boundary condition on solute transport in lysimeters, *Soil Sci. Soc. Am. J.*, *63*, 1493–1499.
Frenkel, H., J. O. Goertzen, and J. D. Rhoades (1978), Effects of clay type and content, exchangeable sodium percentage, and electrolyte concentration on clay dispersion and soil hydraulic conductivity, *Soil Sci. Soc. Am. J.*, *42*, 32–39, doi:10.2136/sssaj1978.03615995004200010008x.
Gasser, M. O., J. Caron, M. R. Laverdière, and R. Lagacé (2002), Solute transport modeling under cultivated sandy soils and transient water regime, *J. Environ. Qual.*, *31*, 1722–1730.
Gonçalves, M. C., J. Šimůnek, T. B. Ramos, J. C. Martins, M. J. Neves, and F. P. Pires (2006), Multicomponent solute transport in soil lysimeters irrigated with waters of different quality, *Water Resour. Res.*, *42*, W08401, doi:10.1029/2005WR004802.
Groenveld, T., A. Ben-Gal, U. Yermiyahu, and N. Lazarovitch (2013), Weather determined relative sensitivity of plants to salinity: Quantification and simulation, *Vadose Zone J.*, *12*(4), 9, doi:10.2136/vzj2012.0180.
Groh, J., J. Vanderborght, T. Pütz, and H. Vereecken (2016), How to control the lysimeter bottom boundary to investigate the effect of climate change on soil processes?, *Vadose Zone J.*, *15*(7), 1–15, doi:10.2136/vzj2015.08.0113.
Hannes, M., U. Wollschläger, F. Schrader, W. Durner, S. Gebler, T. Pütz, J. Fank, G. von Unold, and H. J. Vogel (2015), High-resolution estimation of the water balance of high-precision lysimeters, *Hydrol. Earth Syst. Sci. Discuss.*, *12*, 569–608, doi:10.5194/hessd-12-569-2015.
Hanson, B. R., J. Šimůnek, and J. W. Hopmans (2006), Evaluation of urea-ammonium-nitrate fertigation with drip irrigation using numerical modeling, *Agric. Water Manage.*, *86*, 102–113, doi:10.1016/j.agwat.2006.06.013.
Hanson, B. R., J. W. Hopmans, and J. Šimůnek (2008), Leaching with subsurface drip irrigation under saline, shallow groundwater conditions, *Vadose Zone J.*, *7*(2), 810–818, doi:10.2136/vzj2007.0053.
Hanson, B. R., J. W. Hopmans, and D. E. May (2009), Drip irrigation provides the salinity control needed for profitable irrigation of tomatoes in the San Joaquin Valley, *Calif. Agric.*, *63*(3), 131–136.
Hartz, T. K., and G. J. Hochmuth (1996), Fertility management of drip-irrigated vegetables, *Hort Technol.*, *6*(3), 168–172.
Heinen, M. (2001), FUSSIM2: Brief description of the simulation model and application to fertigation scenarios, *Agronomie*, *21*, 285–296, doi:10.1051/agro:2001124.
Ityel, E., N. Lazarovitch, M. Silberbush, and A. Ben-Gal (2011), An artificial capillary barrier to improve root zone conditions for horticultural crops: Physical effects on water content, *Irrig. Sci.*, *29*(2), 171–180, doi:10.1007/s00271-010-0227-3.
Jacobsen, O. H., F. J. Leij, and M. T. van Genuchten (1992), Lysimeter study of anion transport during steady flow through layered coarse-textured soil profiles, *Soil Sci.*, *154*(3), 196–205.
Jacques, D., C. Smith, J. Šimůnek, and D. Smiles (2012), Inverse optimization of hydraulic, solute transport, and cation exchange parameters using HP1 and UCODE to simulate cation exchange, *J. Contam. Hydrol.*, *142–143*, 109–125, doi:10.1016/j.jconhyd.2012.03.008.
Kaledhonkar, M. J., and A. K. Keshari (2006), Modelling the effects of saline water use in agriculture, *Irrig. Drain.*, *55*, 177–190.
Kandelous, M. M., J. Šimůnek, M. T. van Genuchten, and K. Malek (2011), Soil water content distributions between two emitters of a subsurface drip irrigation system, *Soil Sci. Soc. Am. J.*, *75*(2), 488–497, doi:10.2136/sssaj2010.0181.
Lazarovitch, N., A. Ben-Gal, and U. Shani (2006), An automated rotating lysimeter system for greenhouse evapotranspiration studies, *Vadose Zone J.*, *5*, 801–804, doi:10.2136/vzj2005.0137.
Letey, J., and G. L. Feng (2007), Dynamic versus steady-state approaches to evaluate irrigation management of saline waters, *Agric. Water Manage.*, *91*, 1–10, doi:10.1016/j.agwat.2007.02.014.
Letey, J., G. J. Hoffman, J. W. Hopmans, S. R. Grattan, D. Suarez, D. L. Corwin, J. D. Oster, L. Wu, and C. Amrhein (2011), Evaluation of soil salinity leaching requirement guidelines, *Agric. Water Manage.*, *98*(4), 502–506, doi:10.1016/j.agwat.2010.08.009.
Marek, T., G. Piccinni, A. Schneider, T. Howell, M. Jett, and D. Dusek (2006), Weighing lysimeters for the determination of crop water requirements and crop coefficients, *Appl. Eng. Agric.*, *22*(6), 851–856.
McNeal, B. L. (1968), Prediction of the effect of mixed-salt solutions on soil hydraulic conductivity, *Soil Sci. Soc. Am. J.*, *32*, 190–193, doi:10.2136/sssaj1968.03615995003200020013x.
McNeal, B. L., and N. T. Coleman (1966), Effect of solution composition on soil hydraulic conductivity, *Soil Sci. Soc. Am. J.*, *30*, 308–312, doi:10.2136/sssaj1966.03615995003000030007x.

MDH Engineered Solutions Corp. (2003), *Evaluation of Computer Models for Predicting the Fate and Transport of Salt in Soil and Groundwater*, Edmonton, Alberta, Canada.
Mguidiche, A., G. Provenzano, B. Douh, S. Khila, G. Rallo, and A. Boujelben (2015), Assesing HYDRUS-2D to simulate soil water content (SWC) and salt accumulation under an SDI system: Application to a potato crop in a semi-arid area of central Tunisia, *Irrig. Drain.*, *64*, 263–274.
Neuman, S. P. (1990), Universal scaling of hydraulic conductivities and dispersivities in geologic media, *Water Resour. Res.*, *26*(8), 1749–1758, doi:10.1029/WR026i008p01749.
NOAA-ESRL (2015), Trends in atmospheric carbon dioxide, Earth Syst. Res. Lab., Global Monit. Div., Boulder, Colo. [Available at http://www.esrl.noaa.gov/gmd/ccgg/trends/global.html#global_data.]
Oren, O., Y. Yechieli, J. K. Böhlke, and A. Dody (2004), Contamination of groundwater under cultivated fields in an arid environment, central Arava Valley, Israel, *J. Hydrol.*, *290*, 312–328, doi:10.1016/j.jhydrol.2003.12.016.
Phogat, V., M. Mahadevan, M. Skewes, and J. W. Cox (2012), Modelling soil water and salt dynamics under pulsed and continuous surface drip irrigation of almond and implications of system design, *Irrig. Sci.*, *30*, 315–333, doi:10.1007/s00271-011-0284-2.
Poeter, E. P., M. C. Hill, E. R. Banta, S. Mehl, and S. Christensen (2005), UCODE_2005 and six other computer codes for universal sensitivity analysis, calibration and uncertainty evaluation, *U.S. Geol. Surv. Tech. Methods*, *6-A11*, 283 pp.
Poeter, E. P., M. C. Hill, D. Lu, C. R. Tiedeman, and S. Mehl (2014), UCODE_2014, with new capabilities to define parameters unique to predictions, calculate weights using simulated values, estimate parameters with SVD, evaluate uncertainty with MCMC, and more, *Rep. GWMI 2014-02*, Integ. Groundwater Model. Cent., Golden, Colo.
Raij, I., Lazarovitch, N., Ben-Gal, A., Yermiyhau, U., and Jacques, D. (2013), Accounting for solution composition in a plant roots active nutrient uptake model, in *Proceedings of the 4th International Conference on HYDRUS Software Applications to Subsurface Flow and Contaminant Transport Problems*, edited by J. Šimůnek, M. Th. van Genuchten, and R. Kodešová, pp. 299–306, Dep. of Soil Sci. and Geol., Czech Univ. of Life Sci., Prague, Czech Republic.
Ramos, T. B., J. Šimůnek, M. C. Gonçalves, J. C. Martins, A. Prazeres, N. L. Castanheira, and L. S. Pereira (2011), Field evaluation of a multicomponent solute transport model in soils irrigated with saline waters, *J. Hydrol.*, *407*(1–4), 129–144, doi:10.1016/j.jhydrol.2011.07.016.
Ramos, T. B., J. Šimůnek, M. C. Gonçalves, J. C. Martins, A. Prazeres, and L. S. Pereira (2012), Two-dimensional modeling of water and nitrogen fate from sweet sorghum irrigated with fresh and blended saline waters, *Agric. Water Manage.*, *111*, 87–104, doi:10.1016/j.agwat.2012.05.007.
Rasouli, F., A. K. Pouya, and J. Šimůnek (2012), Modeling the effects of saline water use in wheat-cultivated lands using the UNSATCHEM model, *Irrig. Sci.*, *31*, 1009–1024, doi:10.1007/s00271-012-0383-8.
Raviv, M., and H. J. Lieth (2008), *Soilless Culture: Theory and Practice*, Elsevier B.V., Amsterdam, Netherlands.
Rawlins, S. L. (1973), Principles of managing high frequency irrigation, *Soil Sci. Soc. Am. Proc.*, *37*, 626–629.
Rhoades, J. D., A. Kandiah, and A. M. Mashali (1992), *The Use of Saline Waters for Crop Production*, FAO Irrig. Drain. Pap. 48, Food and Agric. Organ. of the U. N., Rome.
Rhoades, J. D., F. Chanduvi, and S. Lesch (1999), *Soil Salinity Assessment: Methods and Interpretation of Electrical Conductivity Measurements*, FAO Irrig. Drain. Pap. 57, Food and Agric. Organ. of the U. N., Rome.
Roberts, T., N. Lazarovitch, A. W. Warrick, and T. L. Thompson (2009), Modeling salt accumulation with subsurface drip irrigation using HYDRUS-2D, *Soil Sci. Soc. Am. J.*, *73*(1), 233–240, doi:10.2136/sssaj2008.0033.
Ruiz-Peñalver, L., J. A. Vera-Repullo, M. Jiménez-Buendía, I. Guzmán, and J. M. Molina-Martínez (2015), Development of an innovative low cost weighing lysimeter for potted plants: Application in lysimetric stations, *Agric. Water Manage.*, *151*, 103–113, doi:10.1016/j.agwat.2014.09.020.
Russo, D., A. Laufer, R. H. Shapira, and D. Kurtzman (2013), Assessment of solute fluxes beneath an orchard irrigated with treated sewage water: A numerical study, *Water Resour. Res.*, *49*, 657–674, doi:10.1002/wrcr.20085.
Schoen, R., J. P. Gaudet, and D. E. Elrick (1999), Modelling of solute transport in a large undisturbed lysimeter, during steady-state water flux, *J. Hydrol.*, *215*(1–4), 82–93, doi:10.1016/S0022-1694(98)00263-7.
Schröder, N., M. Javaux, J. Vanderborght, B. Steffen, and H. Vereecken (2012), Effect of root water and solute uptake on apparent soil dispersivity: A simulation study, *Vadose Zone J.*, *11*(3), 1–14, doi:10.2136/vzj2012.0009.
Shainberg, I., J. D. Rhoades, and R. J. Prather (1980), Effect of low electrolyte concentration on clay dispersion and hydraulic conductivity of sodic soils, *Soil Sci. Soc. Am. J.*, *45*, 273–277, doi:10.2136/sssaj1981.03615995004500020012x.
Shan, Y., and Q. Wang (2012), Simulation of salinity distribution in the overlap zone with double-point-source drip irrigation using HYDRUS-3D, *Aust. J. Crop Sci.*, *6*(2), 238–247.
Shenker, M., D. Harush, J. Ben-Ari, and B. Chefetz (2011), Uptake of carbamazepine by cucumber plants—A case study related to irrigation with reclaimed wastewater, *Chemosphere*, *82*, 905–910, doi:10.1016/j.chemosphere.2010.10.052.
Silber, A., Y. Israeli, I. Elingold, M. Levi, I. Levkovitch, D. Russo, and S. Assouline (2015), Irrigation with desalinated water: A step toward increasing water saving and crop yields, *Water Resour. Res.*, *51*(1), 450–464, doi:10.1002/2014WR016398.
Silberbush, M., and J. Ben-Asher (2001), Simulation study of nutrient uptake by plants from soilless cultures as affected by salinity buildup and transpiration, *Plant Soil*, *233*, 59–69.
Šimůnek, J., and J. W. Hopmans (2009), Modeling compensated root water and nutrient uptake, *Ecol. Modell.*, *220*(4), 505–521, doi:10.1016/j.ecolmodel.2008.11.004.
Šimůnek, J., and M. T. van Genuchten (2006), Contaminant transport in the unsaturated zone theory and modeling, in *The Handbook of Groundwater Engineering*, edited by J. W. Delleur, pp. 22-1–22-46, CRC Press, Boca Raton.
Šimůnek, J., M. T. van Genuchten, and M. Šejna (2008), Development and applications of the HYDRUS and STANMOD software packages and related codes, *Vadose Zone J.*, *7*(2), 587–600, doi:10.2136/vzj2007.0077.
Šimůnek, J., M. Šejna, and M. Th. van Genuchten (2012), The UNSATCHEM module for HYDRUS (2D/3D) simulating two-dimensional movement of and reactions between major ions in soils, version 1.0, 54 pp., PC Progress, Prague, Czech Republic.
Šimůnek, J., D. Jacques, T. B. Ramos, and B. Leterme (2014), The use of multicomponent solute transport models in environmental analyses, Chapter 16, in *Application of Soil Physics in Environmental Analyses: Measuring, Modelling and Data Integration*, edited by W. Teixeira, et al., pp. 377–402, Springer, Heidelberg, Germany, doi:10.1007/978-3-319-06013-2.
Šimůnek, J., M. T. van Genuchten, and M. Šejna (2016), Recent developments and applications of the HYDRUS computer software packages, *Vadose Zone J.*, *15*(7), 25, doi:10.2136/vzj2016.04.0033.
Skaggs, T. H., and F. J. Leij (2002), Solute transport: Theoretical background, in *Methods of Soil Analysis, Part 4: Physical Methods*, edited by J. H. Dane and G. C. Topp, pp. 1353–1378, Soil Sci. Soc. of Am., Madison, Wis.
Skaggs, T. H., T. J. Trout, J. Šimůnek, and P. J. Shouse (2004), Comparison of HYDRUS-2D simulations of drip irrigation with experimental observations, *J. Irrig. Drain. Eng.*, *130*(4), 304–310, doi:10.1061/(ASCE)0733-9437(2004)130:4(304)CE.

Skaggs, T. H., D. L. Suarez, S. Goldberg, and P. J. Shouse (2012), Replicated lysimeter measurements of tracer transport in clayey soils: Effects of irrigation water salinity, *Agric. Water Manage.*, *110*, 84–93, doi:10.1016/j.agwat.2012.04.003.

Skaggs, T. H., D. L. Suarez, and D. L. Corwin (2014), Global sensitivity analysis for UNSATCHEM simulations of crop production with degraded waters, *Vadose Zone J.*, *13*(6), 1–13, doi:10.2136/vzj2013.09.0171.

Smiles, D. E., and C. J. Smith (2004), Absorption of artificial piggery effluent by soil: A laboratory study, *Aust. J. Soil Res.*, *42*, 961–975, doi:10.1071/SR04008.

Suarez, D. L., and J. Šimůnek (1997), UNSATCHEM: Unsaturated water and solute transport model with equilibrium and kinetic chemistry, *Soil Sci. Soc. Am.*, *61*, 1633–1646.

Tripler, E., U. Shani, A. Ben-Gal, and Y. Mualem (2012), Apparent steady state conditions in high resolution weighing-drainage lysimeters containing date palms grown under different salinities, *Agric. Water Manage.*, *107*, 66–73, doi:10.1016/j.agwat.2012.01.010.

Turkeltaub, T., D. Kurtzman, E. E. Russak, and O. Dahan (2015), Impact of switching crop type on water and solute fluxes in deep vadose zone, *Water Resour. Res.*, *51*, 9828–9842, doi:10.1016/0022-1694(68)90080-2.

Vanclooster, D., M. Mallants, J. Vanderborght, J. Diels, J. Van Orshoven, and J. Feyen (1995), Monitoring solute transport in a multi-layered sandy lysimeter using time domain reflectometry, *Soil Sci. Soc. Am. J.*, *59*, 337–344.

Vanderborght, J., and H. Vereecken (2007), Review of dispersivities for transport modeling in soils, *Vadose Zone J.*, *6*, 29–52, doi:10.2136/vzj2006.0096.

van Genuchten, M. T. (1980), A closed-form equation for predicting the hydraulic conductivity of unsaturated soils, *Soil Sci. Soc. Am.*, *44*(5), 892–898.

van Genuchten, M. T. (1987), A numerical model for water and solute movement in and below the root zone, *Res. Rep. 121*, Riverside, California, USDA, ARS.

van Genuchten, M. T., F. J. Leij, and S. R. Yates (1991), The RETC code for quantifying the hydraulic functions of unsaturated soils, *EPA/600/2-91/065*, pp. 1–85, U.S. Department of Agriculture, Calif., doi:10.1002/9781118616871.

Vrugt, J. A., M. T. van Wijk, J. W. Hopmans, and J. Šimůnek (2001), One-, two-, and three-dimensional root water uptake functions for transient modeling, *Water Resour. Res.*, *37*(10), 2457–2470, doi:10.1029/2000WR000027.

Wang, Q., K. Cameron, G. Buchan, L. Zhao, E. Zhang, N. Smith, and S. Carrick (2012), Comparison of lysimeters and porous ceramic cups for measuring nitrate leaching in different soil types, *N. Z. J. Agric. Res.*, *55*(4), 333–345, doi:10.1080/00288233.2012.706224.

Warrick, A. W., and N. Lazarovitch (2007), Infiltration from a strip source, *Water Resour. Res.*, *43*(3), 1–5, doi:10.1029/2006WR004975.

Weihermüller, L., J. Siemens, M. Deurer, S. Knoblauch, H. Rupp, a Göttlein, and T. Pütz (2007), In situ soil water extraction: A review, *J. Environ. Qual.*, *36*(6), 1735–1748, doi:10.2134/jeq2007.0218.

Winton, K., and J. B. Weber (1996), A review of field lysimeter studies to describe the environmental fate of pesticides, *Weed Technol.*, *10*(1), 202–209.